Istraživanja i projektovanja za privredu
ISSN 1451-4117
DOI:10.5937/jaes0-44452
www.engineeringscience.rs

iipp publishing

Journal of Applied Engineering Science
Vol. 21, No. 4, 2023
Original Scientific Paper
Paper number: 21(2023)4, 1152, 1121-1131

MULTI-PARAMETRIC OPTIMIZATION OF WIRE-EDM MACHINING ON ARTIFICIALLY-AGED AL6061/B_4C COMPOSITE USING RSM AND GREY RELATIONAL ANALYSIS

Subraya Krishna Bhat[1], Shreyas D Sai[2], Gowri Shankar M C[1], Deepak Doreswamy[2]*

[1] *Department of Mechanical and Industrial Engineering, Manipal Institute of Technology, Manipal Academy of Higher Education, Manipal, Karnataka - 576104, India*
[2] *Department of Mechatronics, Manipal Institute of Technology Manipal Academy of Higher Education, Manipal, Karnataka, India-576104*

* *deepak.d@manipal.edu*

Wire-electric discharge machining (W-EDM) is an advanced technology used for machining hard-to-cut materials with high hardness. Therefore, it is critical to characterize and model the Wire-ED machining performance for new materials having remarkable mechanical properties with respect to the multiple control parameters involved in the process. In this light, the present study investigates the multi-parametric optimization of current, pulse-on time (T_{on}), and pulse-off time (T_{off}) on material removal rate (MRR), kerf width (KW), surface roughness (R_a) for Wire-EDM of artificially aged Al6061/B_4C composite using response surface method (RSM) and grey relational analysis (GRA). The results of the investigation revealed that, T_{off} has the most significant impact on the multi-parametric response, with a percentage-wise contribution of 38% from the analysis of variance. The optimization results established that a multi-parametric combination of current – 6 A, T_{on} – 42.5253 µs, and T_{off} – 10 µs achieved the optimum response of MRR – 1.7036 mg/min, KW – 0.1727 mm, and R_a – 5.6525 µm. The results obtained herewith have practical relevance to Wire-EDM industry for manufacturing applications.

Keywords: Wire-EDM, Al6061/B_4C, grey relational analysis, pulse-on time, pulse-off time, current

1 INTRODUCTION

Aluminium alloy-based metal matrix composites impregnated with harder reinforcement materials such as Boron Carbide (B_4C) have gained significant attention by the scientific community due to their attractive physical, mechanical and thermal properties which make them suitable for a wide array of engineering applications such as the transportation and storage of spent nuclear fuel [1,2], armours in defence industry [3] and aerospace, automotive and marine industrial products. The low density (2.52gm/cm^2) B_4C particles considered to be one of the hardest materials, which retains a high degree of thermal, chemical, electrical and mechanical properties, resulting in an attractive reinforced material to improve the properties of aluminium-based composites. Very limited research has been observed on aluminium alloy composites reinforced with B_4C particles because of its expensiveness, poor wettability and complication of manufacturing of composites [4]. In addition, Al_2O_3, SiC, TiC and ZnO reinforced composites also show superior fatigue strength, fracture-resistance and good strength-to-weight ratio [4,5]. The specific strength of these composites is further enhanced by age or precipitation hardening [6] in which the material undergoes microstructural realignment in the aluminium (Al-Mg-Si) matrix [5]. In Al6061-B_4C composites, the aluminum matrix is strengthened through the formation of fine precipitates during precipitation hardening, which can increase the overall strength of the composite. This is especially important when using composite materials in applications where hardness, wear resistance, strength and fatigue resistance is a critical factor, making the composite even more suitable for various applications. One potential drawback of precipitation hardening is a reduction in ductility. This means that the material may become less able to deform plastically before fracture. In some applications, this reduction in ductility may be acceptable, but it should be considered in designs where ductility is essential. During precipitation hardening, the microstructure of the composite material evolves as precipitates form. This can lead to changes in the material's properties, including grain size, distribution of B_4C particles, and dislocation density. These changes can affect the overall performance of the composite. This results in improving their specific strength and wear resistance [7,8] which subsequently affects the machinability of the composite by the conventional machining methods [8]. In this regard, non-traditional metal cutting technologies such as wire electric discharge machining (WEDM), Laser machining, chemical machining, etc., have emerged as suitable candidates for the machining of such hard materials [9].

Wire EDM is an advanced machining technology comprising of electro-chemical processes which cuts the materials through the application of rapid and repetitive electrical sparks at high frequencies. The intensity of concentrated heat energy produced by these electrical sparks generates extremely high temperatures ranging up to 10,000°C [10] in the localized region which results in melting or evaporation of the workpiece material. The dielectric fluid such as deionized water, is circulated around the workpiece to conduct the electrical discharges also flushes away the debris of the molten material machined from the base workpiece. The performance of Wire-EDM is measured by parameters such as material removal rate (MRR), surface finish (R_a), kerf width (KW), are influenced by the machining parameters such as pulse on time (T_{on}), pulse off time (T_{off}), current, voltage and wire feed rate, wire tension [10].

The choice of electrode material and the machining environment, i.e., the dielectric fluid medium plays an important part in the wire EDM process. The brass wire electrode materials are preferred by most researchers for machining of Al6061 based metal matrix composites [11-14] compared to copper [15,16] and molybdenum [5,9] wires. However, in case of the dielectric fluid media there has been a near consensus in the literature on using deionized (also called demineralized) water for the ionisation, flushing and cooling purposes [5,9,11-14].

Literature shows that various ranges of T_{on} i.e., 6 µs – 10 µs [11,15], 20 µs – 80 µs [9,12,16] and much higher values of 106 µs – 126 µs [14] have been used for machining of Al6061 composites. The range of T_{off} has been chosen around 4 µs – 10 µs [11,12,16] or much higher values around 45 µs – 55 µs [14]. The present work employs molybdenum wires as the electrode material and deionized water for the investigation. Current, T_{on} and T_{off} were chosen as the operating parameters for the optimization. The range of T_{on} has been chosen as 30 µs – 50 µs, T_{off} as 10 µs – 20 µs which has been found to give reasonable results in research on WED machining of Al6061 as well as other metals [5,10]. Also, the present study was carried out at low current settings in the range of 4 A – 6 A which could be useful for machining with lower requirements of current [9,13].

Wire-EDM is a potential candidate among non-traditional techniques for machining of hard materials. Since there exists a range of WEDM machining parameters under which the machining could be conducted, it is of paramount importance to arrive at the optimum values of their settings to obtain a desirable machining output performance. With this objective in place, various researchers have investigated various methods of optimization such as response surface method (RSM) [17,18], Taguchi technique [19], grey relational analysis (GRA) [20-22] for the process optimization and modeling of WEDM of various materials. However, there is a paucity of application of GRA technique in case of WED machining of Al6061 reinforced metal matrix composite [23]. According to the best knowledge of the authors', the present study is the first such investigation, especially for age-hardened Al6061/B_4C composite. In this study, machining experiments were carried out with variations of the critical control parameters of current, T_{on} and T_{off} while the obtained MRR, kerf width (KW), and surface roughness (R_a) values were measured for each trial. The obtained experimental data was subjected to analysis of variance, GRA, and regression modeling.

2 MATERIALS AND METHODS

2.1 Fabrication of Al6061/B_4C composite

The B_4C particles were prepared by cleansing them in an ultrasonic agitator using distilled water, to get rid of deposited fine particles on their surface. The cleansing process was carried out four times for a period of 10 to 15 minutes in the agitator, the distilled water being replaced in each cleansing cycle. After cleansing with distilled water, the B_4C particles were cleansed with acetone using the ultrasonic agitator. After the cleansing processes, the reinforcement particles were preheated at 250°C for 2 hours for eliminating the presence of volatile compounds, removing residual impurities and to improve their wettability [5,24]. The fabrication process of Al6061/B_4C composites begins with the melting of Al6061 billets (composition provided in Table 1) in a crucible using a 5-kW electric furnace at a constant temperature of 750°C. Slag generated in this process are removed by adding a small amount of scum powder. Degassing of molten melt is carried out by adding 10 grams of dry hexachloroethane (C_2Cl_6) [25]. After cooling the composite melt to a temperature of 600°C, a semi-solid state is reached, during which the preheated reinforcement particles are slowly introduced into the vortex of molten metal being stirred in the stirrer (Figure 1(a)). The stirring is continued for a period of 10 minutes at around 200 rpm. Subsequently, the stirring is continued at 750°C for a period of 10 more minutes at 400 rpm. The molten composite is then poured into cast iron moulds which are maintained at a temperature of 500°C (Figure 1(b)). The cast samples are then subjected to artificial aging by solutionizing at 558°C for 2 hours and later quenching in demineralised water at 25°C. Further, a second cycle of artificial aging, the samples are subjected to a furnace at 100°C for 8 hours [5,24].

Table 1. Composition (wt.%) of Al6061 [5]

Material	Si	Fe	Cu	Mn	Zn	Ti	Mg	Cr	Al
Wt. %	0.50	0.55	0.25	0.14	0.24	0.12	0.95	0.20	Remaining

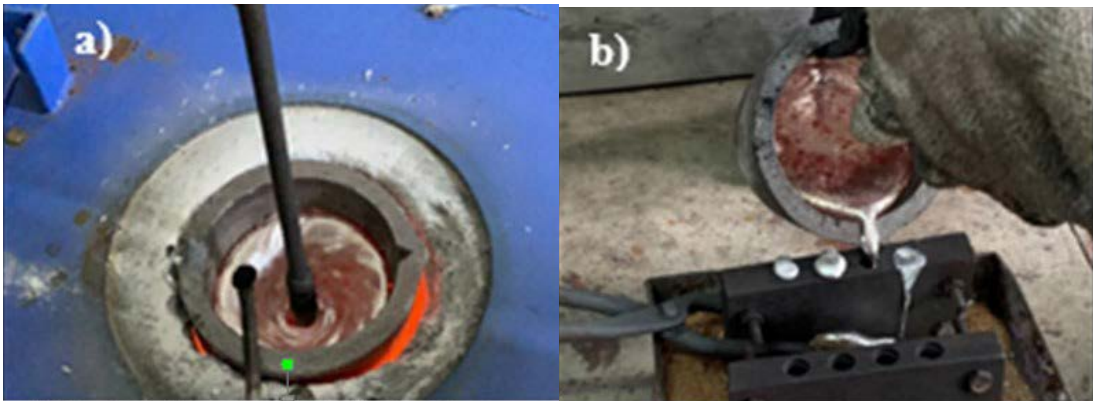

Fig. 1. (a) Stirring process and (b) pouring of molten composite into preheated die [5]

2.2 Experimental plan

Experiments were conducted on a 2-axis (X-320 mm, Y-400 mm) CNC wire-EDM made by Concord wire-EDM (Model: DK7732). Electrode made of molybdenum wire (0.16 mm diameter) is employed. A mixture of soft water and gel is employed as the dielectric fluid. Critical parameters such as, T_{on}, T_{off} and current were chosen for optimization in the current study. The levels of process parameters were designed using L_{20} RSM using the central composite approach of experimental design. The design consists of total 40 experimental trials with different combinations of T_{on}, T_{off} and current (Table 2). During these experiments, the supply pressure, voltage and wire speed were kept constant. In total, 40 slots were cut in the specimen using the different parametric combinations listed in Table 2.

Table 2. Experimental plan

Exp. No.	Current (A)	T_{on} (µs)	T_{off} (µs)	MRR (mg/min)	R_a (µm)	KW (mm)
1	6	30	10	1.85	6.29	0.18
2	4	50	10	1.33	6.36	0.16
3	5	40	15	0.74	5.34	0.16
4	4	30	20	0.28	5.69	0.16
5	6	50	20	0.70	6.51	0.17
6	5	30	15	0.74	6.10	0.17
7	5	40	15	0.81	5.87	0.18
8	4	40	15	0.50	6.19	0.17
9	6	40	15	0.83	6.13	0.17
10	4	50	20	0.42	6.58	0.19
11	5	40	15	0.69	6.08	0.16
12	5	40	15	0.62	6.41	0.14
13	5	40	15	0.84	5.74	0.18
14	6	30	20	0.68	6.95	0.18
15	5	40	20	0.49	6.73	0.18
16	5	40	10	1.48	5.29	0.17
17	4	30	10	1.12	6.67	0.16
18	6	50	10	1.56	6.26	0.16
19	5	40	15	0.78	6.94	0.17
20	5	50	15	0.79	5.70	0.17
21	5	40	15	0.84	7.18	0.18
22	5	40	15	0.83	6.34	0.18
23	5	40	15	0.71	5.25	0.15
24	5	40	15	0.80	6.37	0.17
25	5	30	15	0.77	6.76	0.17
26	4	50	20	0.40	5.77	0.17
27	6	40	15	0.59	7.30	0.16
28	5	50	15	0.80	6.79	0.17
29	6	50	20	0.62	7.29	0.15
30	5	40	10	1.78	5.47	0.19
31	4	50	10	1.34	6.29	0.17
32	6	30	10	1.65	6.07	0.17
33	6	30	20	0.65	6.00	0.16
34	4	30	10	1.17	6.13	0.16
35	4	40	15	0.64	5.39	0.16

Exp. No.	Current (A)	T_{on} (µs)	T_{off} (µs)	MRR (mg/min)	R_a (µm)	KW (mm)
36	5	40	15	0.82	6.85	0.18
37	6	50	10	1.82	7.14	0.18
38	5	40	15	1.60	6.56	0.18
39	5	40	20	0.79	5.52	0.17
40	4	30	20	0.31	5.70	0.17

2.3 Measurement of responses

Test samples machined according to the plan listed in Table 2 were then analysed to evaluated the material removal rate (MRR) achieved during machining. The MRR achieved during each trial is computed using the weight loss technique, measuring the reduction in weight per unit time as described by Equation 1. A digital weighing unit was used to determine the initial and final weights of the workpiece, that is, before and after machining.

$$MRR = \frac{W_i - W_f}{t}, \text{mg/min} \quad (1)$$

Further, the surface roughness (R_a) were measured using the surface roughness tests (Surtronic: Taylor-Hobson, Leicester, England). The measurements were taken at three locations along the length of the cut and the average value was recorded. Finally, the slots were investigated for the kerf width (KW) with different parametric combinations. The kerf/slot were measured using the Inverted Metallurgical Optical Microscope (IM7000 Series: Mitutoyo, Meiji Techno, Japan) at two locations, one near the beginning, and another one near the end of the slot; and the average value was recorded. In summary, the values of MRR, R_a, and KW measured as the machining responses are shown in Table 2.

2.4 Grey relational analysis

Popular experimental design techniques such as Taguchi and RSM have been used for single response optimization of machining performance. However, grey relational analysis (GRA) is a promising tool in case of multi-response or multi-criteria decision-making problems such as the present scenario, wherein, the three responses, i.e., MRR, R_a, and KW need to be optimized with respect to the given range of input parameters, i.e., current, T_{on}, and T_{off}. For the best machining performance, MRR needs to be maximized, and R_a and KW are to be minimized. The grey relational analysis method is outlined in Figure 2. Here, “grey” indicates that the available information is insufficient to make a black or white decision; and hence utilizing the partial information available, denoted as “grey”, the analysis is conducted to achieve the optimum performance [20-22].

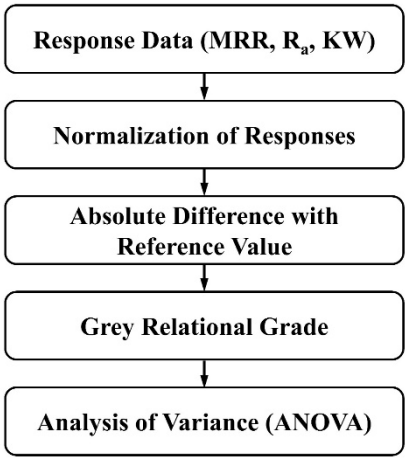

Fig. 2. The steps involved in GRA

3 RESULTS AND DISCUSSION

3.1 Computation of grey-relation: normalization of responses

For a normalized evaluation of the effects of the measured responses, the actual values used in the experiments are normalized linearly between zero and one (Table 3). The normalization ensures that the response data is distributed proportionately according to their actual values, their qualitative and quantitative variations with respect to control parameters. The normalization is carried out according to two scenarios: in case of MRR, which needs to be maximized, the “higher-the-better” characteristic is obtained using Equation 2, in case of R_a and KW, which need to be minimized, the “smaller-the-better” condition is attained using Equation 3.

$$X_{ijk*} = \frac{Max(X_{ijk}) - X_{ijk}}{Max(X_{ijk}) - Min(X_{ijk})}, j = 1,2,...40 \quad (2)$$

$$X_{ijk*} = \frac{X_{ijk} - Min(X_{ijk})}{Max(X_{ijk}) - Min(X_{ijk})}, j = 1,2,...40 \quad (3)$$

Table 3. Computed grey relational values

Exp. No.	Normalized Responses			Grey Relational Coefficient			Grey relational grade
	MRR	R_a	KW	MRR	R_a	KW	
1	1.00	0.65	0.17	1.00	0.48	0.29	0.589
2	0.67	0.59	0.57	0.50	0.44	0.43	0.459
3	0.30	0.96	0.65	0.32	0.89	0.49	0.566
4	0.00	0.79	0.65	0.25	0.61	0.49	0.450
5	0.27	0.32	0.48	0.31	0.33	0.39	0.341
6	0.30	0.47	0.35	0.32	0.38	0.34	0.346
7	0.34	0.56	0.22	0.33	0.43	0.30	0.352
8	0.14	0.68	0.35	0.28	0.51	0.34	0.373
9	0.35	0.80	0.48	0.34	0.63	0.39	0.451
10	0.09	0.71	0.13	0.27	0.53	0.28	0.359
11	0.27	0.55	0.65	0.31	0.42	0.49	0.407
12	0.22	0.79	1.00	0.30	0.61	1.00	0.637
13	0.36	0.82	0.17	0.34	0.65	0.29	0.425
14	0.25	0.43	0.26	0.31	0.36	0.31	0.327
15	0.14	0.51	0.17	0.28	0.40	0.29	0.322
16	0.76	0.66	0.39	0.58	0.49	0.35	0.476
17	0.54	0.55	0.61	0.42	0.42	0.46	0.433
18	0.81	0.64	0.65	0.64	0.48	0.49	0.536
19	0.32	0.21	0.39	0.33	0.30	0.35	0.325
20	0.33	0.77	0.43	0.33	0.59	0.37	0.429
21	0.36	0.31	0.17	0.34	0.32	0.29	0.316
22	0.35	0.34	0.22	0.34	0.33	0.30	0.322
23	0.28	1.00	0.70	0.31	1.00	0.52	0.611
24	0.33	0.25	0.35	0.33	0.30	0.34	0.324
25	0.31	0.49	0.39	0.32	0.39	0.35	0.356
26	0.08	0.69	0.35	0.26	0.52	0.34	0.372
27	0.20	0.00	0.52	0.29	0.25	0.41	0.316
28	0.33	0.09	0.43	0.33	0.27	0.37	0.322
29	0.22	0.16	0.74	0.30	0.28	0.56	0.379
30	0.96	0.74	0.00	0.88	0.56	0.25	0.562
31	0.67	0.26	0.39	0.50	0.31	0.35	0.388
32	0.87	0.68	0.43	0.72	0.51	0.37	0.534
33	0.24	0.64	0.52	0.30	0.48	0.41	0.397
34	0.57	0.12	0.61	0.43	0.27	0.46	0.388
35	0.23	0.88	0.52	0.30	0.73	0.41	0.480
36	0.35	0.51	0.30	0.34	0.40	0.32	0.354
37	0.98	0.25	0.22	0.95	0.31	0.30	0.519
38	0.84	0.36	0.30	0.68	0.34	0.32	0.447
39	0.33	0.63	0.43	0.33	0.47	0.37	0.389
40	0.02	0.57	0.39	0.25	0.44	0.35	0.347

3.2 Computation of grey-relational coefficient

The normalized responses are used in the computation of the grey relational coefficient (GRC) which formulates the relationship between normalized and actual values of experimental responses. This is obtained by using the Equations 4 and 5. Here, we consider all responses to be of equal importance and hence, the characteristic coefficient (ξ) is considered to be 1/3, thus taking an unweighted averaged value from each machining response [20-22]. Table 3 provides the computed GRC values.

$$V_{ijk} = \left| X_{ijk*} - Max(X_{ijk*}) \right| \tag{4}$$

$$\xi_{ijk*} = \frac{Min(V_{ijk}) + \xi Max(V_{ijk})}{V_{ijk} + \xi Max(V_{ijk})} \tag{5}$$

3.3 Computation of grey-relational grade

The final calculation in the multi-criteria decision-making approach of GRA is obtaining the grey relational grade (GRG). This provides a composite multi-factorial relationship among the responses and provides a numerical grading by which the best machining combination can be identified. It is an averaged value of the GRC values computed previously, as shown in Equation 6. The calculated values of GRG are tabulated in Table 3.

$$GRG = \frac{1}{3}\sum_{i=1}^{3} GRC \tag{6}$$

3.4 Main effects of Current, T_{on}, and T_{off} on Grey-Relational Grade

Figure 3 shows the main effects plot of current, T_{on}, and T_{off} on GRG. It is observed that GRG increases with current from 4 A to 6 A, with a rise of 8.4%. This is explained due to the fact that, higher current settings lead to higher electro-thermal energy transfer to the base material which causes higher MRR, better surface finish and a smoother cut slots/kerf. With regards to T_{on}, there is a marginal change in GRG, with a maximum variation in GRG of 3.1%. As T_{on} increases there is a higher amount of current energy being supplied to the workpiece; however, the results suggest that within the range of current being supplied, there is a negligible apparent influence on the GRG with change in time duration of T_{on}. However, a significant change in GRG of 32.7% is observed with respect to T_{off} duration from 10 µs to 20 µs, with the maximum GRG being observed at 10 µs. As T_{off} increases, the time duration between subsequent electric pulses increases thereby leading to lesser material removal and also hampering the other responses. Therefore, here, it is observed that, the minimum T_{off} settings provide the optimal multi-parametric response.

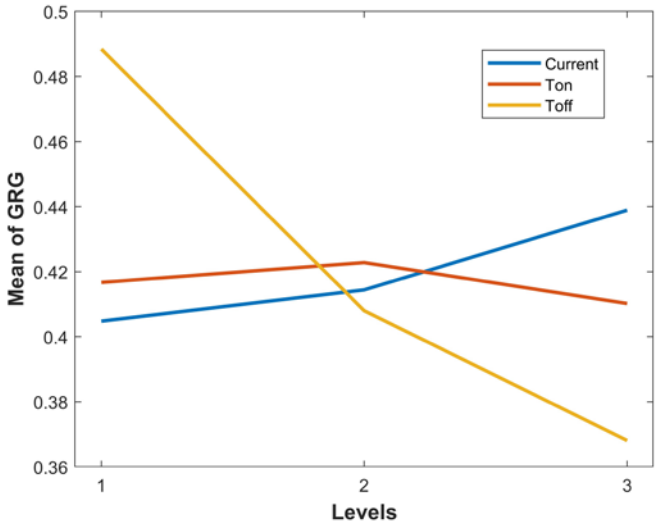

Fig. 3. Main effect plot of GRG

3.5 Interaction effects of Current, T_{on}, and T_{off} on Grey-Relational Grade

Figure 4 shows the interaction effect plots of current, T_{on}, and T_{off} on GRG in the form of response surfaces, with Z-axis being the combined effect of the three machining responses. From Figure 4a it is observed that, the maximum GRG is obtained at the minimum T_{on} and maximum current settings, i.e., at 30 µs and 6 A. At maximum current settings, since the maximum electro-thermal discharge is being supplied, the higher values of time could hamper the surface quality in terms of roughness and kef width. Therefore, the optimum value of time duration to obtain best possible trade-off for the three machining responses. The interaction effect of T_{on} and T_{off}, on GRG is shown in Figure 4b. It is found that, the minimum settings of both T_{on} and T_{off} achieves the best GRG. This can be analysed in conjunction with the results of main effect plot of Figure 3. Since T_{off} showed a more prodigious effect on GRG, and

increasing T_{on} did not make significant change in GRG, it can be extended that, a combined effect of T_{on} and T_{off} would result in best combinatorial effect at the minimum T_{off} and T_{on} setting. At this setting, with the 5 A current value, the best GRG is obtained. The interaction effects of current and T_{off} is presented in Figure 4c. Here, it is observed that the best GRG response is obtained at the maximum current and minimum T_{off} setting. At the maximum current setting, the maximum discharge energy is impacting on the workpiece. If this condition is maintained for a longer time duration, it could lead to greater material removal; however, also leading to excessive kerf widths.

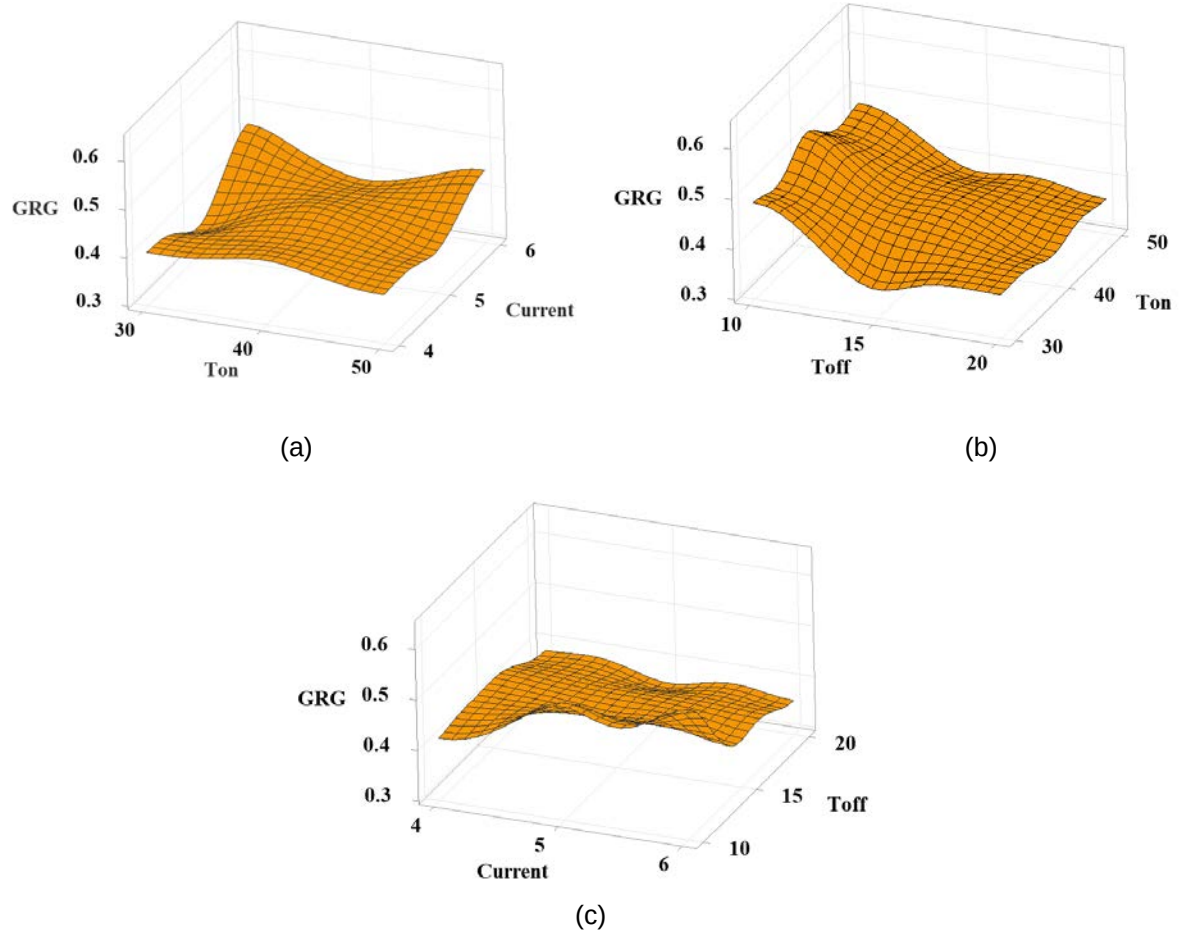

Fig. 4. Interaction effects of (a) Current and T_{on}, (b) T_{on} and T_{off}, and (c) T_{off} and Current on GRG

3.6 Analysis of variance of Grey-Relational Grade

Table 4 presents the ANOVA of GRG with respect to the control parameters with a confidence interval of 95%. To evaluate the statistical significance of the control parameters on to the GRG, the critical F-statistic or variance ratio is obtained from the standard Fisher (F) distribution table. The critical F-statistic for the degree of freedom (DF) of the control parameters and the error DF ($F_{0.05(1,30)}$) is 4.17. From the ANOVA table, it is observed that only Toff shows a statistically significant and prominent effect on GRG, since its F-value > $F_{0.01(1,30)}$ with a P-value of 0.003. In comparison, the other prominent effect is that of the combinatorial effect of Current and T_{off}, with an F-value of 3.15 which is close to the statistical critical value. This characteristic is also consistent with the observation of the response surface plot shown in Figure 4, since there appears a sudden peak observed in GRG with the maximum current and minimum T_{off} settings. Additionally, for a qualitative evaluation of the percentage contribution of the individual parameter on the GRG, the % mean of squares is shown in Table 4. The significant effects of T_{off} and interaction effects of Current and T_{off}, is clearly demonstrated in terms of their % MS, which are one order larger than the effects of other individual parameters or combinatorial/quadratic effects [26,27].

Table 4. ANOVA of GRG

Source	DF	Adj SS	Adj MS	F-Value	P-Value	% MS
Model	9	0.111980	0.012442	1.78	0.115	6.5
Linear	3	0.078263	0.026088	3.72	0.022	13.7
Current	1	0.005801	0.005801	0.83	0.370	3.0
T_{on}	1	0.000207	0.000207	0.03	0.865	0.1
T_{off}	1	0.072255	0.072255	10.31	0.003	38.0

Source	DF	Adj SS	Adj MS	F-Value	P-Value	% MS
Square	3	0.011535	0.003845	0.55	0.653	2.0
Current*Current	1	0.000206	0.000206	0.03	0.865	0.1
T_{on}*T_{on}	1	0.007084	0.007084	1.01	0.323	3.7
T_{off}*T_{off}	1	0.007995	0.007995	1.14	0.294	4.2
2-Way Interaction	3	0.022181	0.007394	1.05	0.383	3.9
Current*T_{on}	1	0.000068	0.000068	0.01	0.922	0.0
Current*T_{off}	1	0.022067	0.022067	3.15	0.086	11.6
T_{on}*T_{off}	1	0.000046	0.000046	0.01	0.936	0.0
Error	30	0.210290	0.007010			3.7
Lack-of-Fit	20	0.066477	0.003324	0.23	0.997	1.7
Pure Error	10	0.143813	0.014381			
Total	39	0.322270				

The influence of the different parameters on GRG is also presented in terms of a Pareto chart of the standardized effects (see Figure 5). The Pareto chart shows an ordered list of parameters according to their significance on the multi-parametric machining response. It is found that, parameter T_{off} is the most significant parameter, followed by the interaction of Current and T_{off} which is in line with the ANOVA results, as depicted by the F-ratio value of these parameters in Table 4. These l are followed by the quadratic effects of Toff, Ton, and individual effect of Current. Other individual and combinatorial effects are showing comparatively infinitesimal impacts on the GRG, consequently on the multi-parametric machining response.

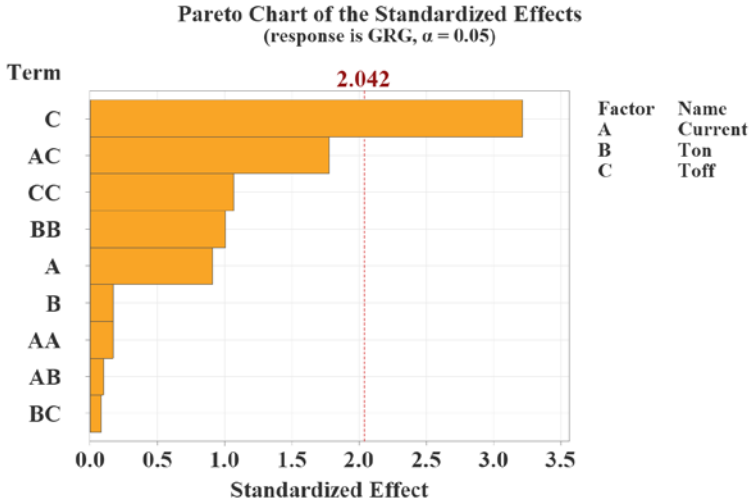

Fig. 5. Pareto chart of the standardized effects on GRG

3.7 Multi-parametric optimization

The mean response of GRG with respect to the different levels of the control parameters utilized in the experiments, is listed in the Table 5. The mean response table, with the maximum GRG obtained using different combinations of the control parameters, exemplifies the best possible and worst possible parametric combinations on the multi-response. The best possible multi-characteristic response for different control parameters is represented in boldface, i.e.., Current at level 3, T_{on} at level 2, and T_{off} at level 1 provide the best GRG. From a combinational perspective, the combination of $A_3B_2C_1$ (where, A – Current, B – T_{on}, and C – T_{off}) is identified as the best one, while that of $A_1B_3C_3$ is the worst of the lot.

Table 5. Mean GRG response with respect to control parameter levels

Parameter	Level 1	Level 2	Level 3
Current	0.4048	0.4144	**0.4389**
T_{on}	0.4167	**0.4228**	0.4102
T_{off}	**0.4884**	0.4080	0.3681

Composite desirability is a statistical measure which encapsulates the overall optimal performance or machining response taking account of all the factors under investigation. Using this perspective of composite desirability on

GRG and the control parameters, the multi-parametric response optimization is depicted in Figure 6. Here, a composite desirability of 0.6299 is achieved which is comparable to those obtained for Wire-EDM optimization for other hard-to-cut materials [22,28]. The obtained optimum combination of control parameters revealed that, Current is at level 3, which is same as the observation in Table 5. Further, T_{on} is close to and above level 2 (see Table 5), which can be understood as a trade-off to achieve the multi-response optimization. Finally, Toff is at level 1, which is again matching with the expected optimum condition according to their individual effects. Therefore, with a minor deviation from their individual optimum conditions, a multi-parametric optimized condition is derived employing the grey-relational technique of analysis and optimization, yielding an MRR of 1.7036 mg/min, KW of 0.1727 mm, and R_a of 5.6525 µm. These optimized responses are comparable with similar studies on GRA approach-based optimization of Wire-EDM for different materials [22,26].

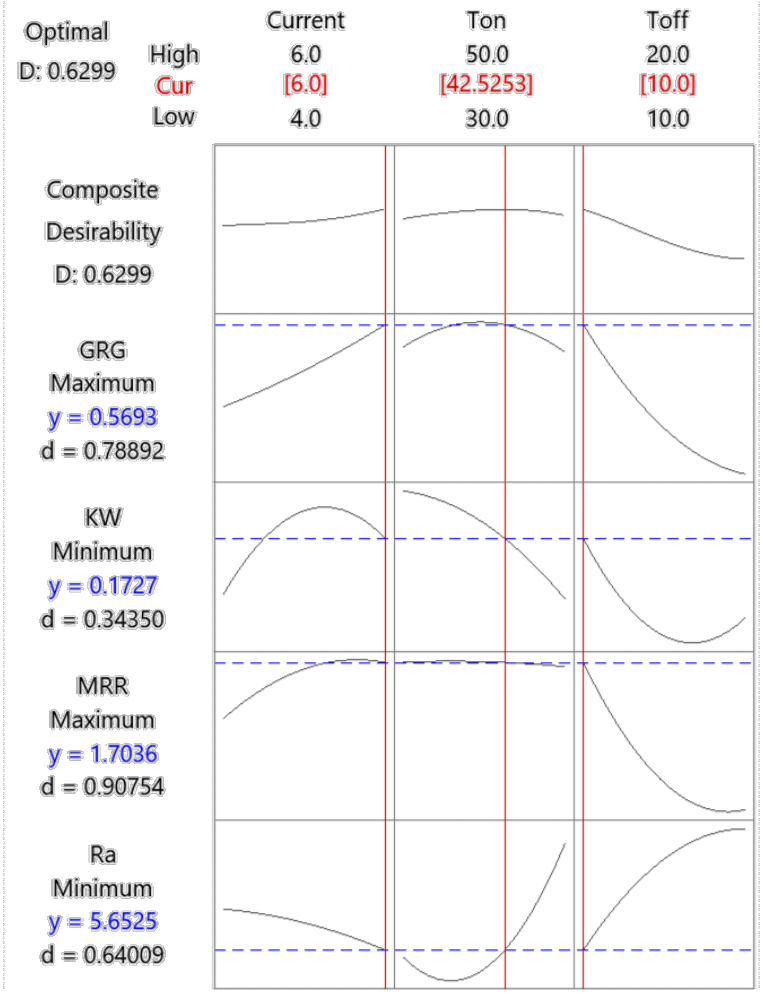

Fig. 6. Optimization plot considering the composite desirability, GRG and the machining responses.

Overall, it is observed that the maximized MRR, and minimized KW and R_a is achieved with the Level 1 of T_{off}, Level 2 of T_{on} and Level 3 of current, respectively. As T_{on} increases, amount of MRR increases, but also resulting in a deterioration of surface roughness and increase in kerf width. With increase in Current, a better surface roughness and MRR can be achieved. With increase in T_{off}, there will be a drop in MRR, having a negative impact on the machining process. Therefore, a lower T_{on}, higher current and intermediate level of T_{on} is achieving the multi-response optimization.

4 CONCLUSIONS

In this study, the versatile and powerful RSM-GRA technique was employed for the multi-parametric optimization of Wire-ED machining of Al6061/B_4C composite. The conclusions of this study are listed herein:

1. The main effect analysis of the control parameters revealed that, T_{off} has the most significant impact on grey relational grade (inducing 32.7% increase from 20 µs to 10 µs), followed by Current and T_{on}.
2. The interaction effect analysis based on response surfaces revealed that, the maximum GRG is obtained at the combinations of T_{on} – 30 µs and Current – 6 A, T_{on} – 30 µs and T_{off} – 10 µs, and T_{off} – 10 µs and Current – 6 A.
3. ANOVA results along with investigation of Pareto chart established the prominent influence of T_{off}, individually, and Current and T_{off}, as a combination, with percentage contributions of 38% and 11.6%, respectively.

4. The mean GRG response showed that, the effects of the control parameters can be ranked according to their influence on the multi-parametric response as: T_{off} – I, Current – II, and T_{on} – III.
5. The GRA based multi-parametric optimization with consideration of composite desirability as the statistic parameter established that the parameter combinations of: Current – 6 A, T_{on} – 42.5253 µs, and T_{off} – 10 µs provides the optimum response, yielding an MRR – 1.7036 mg/min, KW – 0.1727 mm, and R_a – 5.6525 µm. These results are valid with their range of values considered in the present study (4 A ≤ Current ≤ 6 A, 30 µs ≤ T_{on} ≤ 50 µs, 10 µs ≤ T_{on} ≤ 20 µs).

5 REFERENCES

[1] Sakaguchi, Y., Saida, T., Kuri, S., Ohsono, K., Hode, S., Matsuoka. T. (2022). Development of High Capacity Transportable Storage Cask for Basket. *The Proceedings of the National Symposium on Power and Energy Systems*, vol. 8, 449-450, DOI: 10.1299/jsmepes.2002.8.449

[2] Yamamoto, T., Hode, S., Kamiwaki, Y., Tamaki, H., Matsuoka, T., Hojo. K. (2006). Developments in Spent Fuel Transport and Storage Casks, Mitsubishi Heavy Industries, Ltd. Technical Review, vol. 43, no. 4, from *https://www.mhi.co.jp/technology/review/pdf/e434/e434050.pdf*

[3] Chand, S., Chandrasekhar. P., (2020). Influence of B4C/BN on solid particle erosion of Al6061 metal matrix hybrid composites fabricated through powder metallurgy technique. *Ceram. Int*. vol. 46, no. 11, 17621-17630, DOI: 10.1016/j.ceramint.2020.04.064

[4] Karabulut, Ş., Karakoç, H., Çıtak. R., Influence of B4C particle reinforcement on mechanical and machining properties of Al6061/B4C composites. *Compos Part B: Eng*, vol. 101, no. 15, 87-98, DOI: 10.1016/j.compositesb.2016.07.006

[5] Doreswamy, D., Gowrishankar, M.C., Sai. S.D. (2022). Investigation on the Wire Electric Discharge Machining Performance of artificially aged Al6061/B4C composites by Response Surface Method. *Mater. Res*. vol. 25, e20220010, DOI: 10.1590/1980-5373-MR-2022-0010

[6] Gowrishankar, M.C., Hiremath, P., Shettar, M., Sharma, S.S., Rao. S.U. (2020). Experimental validity on the casting characteristics of stir cast aluminium composites. J Mater Res Technol. vol. 9, no. 3, 3340-3347, DOI: 10.1016/j.jmrt.2020.01.028

[7] Y.C. Shin, C. Dandekar. Mechanics and Modeling of Chip Formation in Machining of MMC. In: Davim, J. (eds) Machining of Metal Matrix Composites. Springer, London. (2012)

[8] Shettar, M., Hiremath, P., Shankar, G., Kini, A., Sharma. S.S. (2021). Tribolayer Behaviour and Wear of Artificially Aged Al6061 Hybrid Composites. *Int J Automot Mech Eng*. vol. 18, no. 2, 8668–8676, DOI: 10.15282/ijame.18.2.2021.04.0660

[9] Doreswamy, D., Bongale, A.M., Piekarski, M., Bongale, A., Kumar, S., Pimenov, D.Y., Giasin, K., Nadolny, K. (2021). Optimization and Modeling of Material Removal Rate in Wire-EDM of Silicon Particle Reinforced Al6061 Composite. *Materials*, vol. 14, no. 21, 6420, DOI: 10.3390/ma14216420

[10] Doreswamy, D., Sai, S.D., Bhat, S.K., Rao. R.N. (2022). Optimization of material removal rate and surface characterization of wire electric discharge machined Ti-6Al-4V alloy by response surface method. *Manuf Rev*. vol. 9, 15, DOI: 10.1051/mfreview/2022016

[11] Satishkumar, D., Kanthababu, M., Vajjiravelu. V. (2011). Investigation of wire electrical discharge machining characteristics of Al6063/SiCp composites. *Int J Adv Manuf Technol*., vol. 56, 975–986. DOI: 10.1007/s00170-011-3242-5

[12] Babu, K.A., Venkataramaiah. P. (2015). Multi-response Optimization in Wire Electrical Discharge Machining (WEDM) of Al6061/SiCp Composite Using Hybrid Approach. *J Manuf Sci Prod*., vol. 15, no. 4, 327-338, DOI: 10.1515/jmsp-2015-0010

[13] Mythili, T., Thanigaivelan. R. (2020). Optimization of wire EDM process parameters on Al6061/Al2O3 composite and its surface integrity studies. *Bulletin Pol Acad Sci Tech Sci*., vol. 68, no. 6, 1403-1412, DOI: 10.24425/bpasts.2020.135382

[14] Velmurugan, N., Muniappan, A., Harikrishna, K.L., Sakthivel. T.G. (2021). Surface roughness modelling in wire EDM machining aluminium of Al6061 composite by ANFIS. *Mater Today: Proc*., DOI: 10.1016/j.matpr.2021.07.119

[15] Dey, A., Debnath, S., Pandey. K.M. (2017). Optimization of electrical discharge machining process parameters for Al6061/cenosphere composite using grey-based hybrid approach. *Trans. Nonferrous Met. Soc. China*., vol. 27, 998−1010, DOI: 10.1016/S1003-6326(17)60117-1

[16] Sreeram, H., Uthayakumar, M., Kumar, S.S., Kumaran, S.T., Korniejenko. K. (2022). Modelling Approach for the Prediction of Machinability in Al6061 Composites by Electrical Discharge Machining. *Appl Sci*., vol. 12, no. 5, 2673, DOI:

[17] Arikatla, S.P., Mannan, K.T., Krishnaiah. A. (2017). Parametric optimization in wire electrical discharge machining of titanium alloy using response surface methodology. *Mater. Today: Proc*., vol. 4, 1434–1441, DOI: 10.1016/j.matpr.2017.01.165

[18] Fuse, K., Dalsaniya, A., Modi, D., Vora, J., Pimenov, D.Y., Giasin, K., Prajapati, P., Chaudhari, R., Wojciechowski, S. (2021). Integration of fuzzy AHP and fuzzy topsis methods for wire electric discharge machining of titanium (Ti6Al4V) alloy using RSM. *Materials*, vol. 14, 7408, DOI: 10.3390/ma14237408

[19] Daneshmand. S., Kahrizi, E.F., LotfiNeyestanak, A.A., Monfared, V. (2014). Optimization of electrical discharge machining parameters for Niti shape memory alloy by using the Taguchi method. *J. Marine Sci. Technol*., vol. 22, 506–512, DOI: 10.6119/JMST-013-0624-1

[20] Doreswamy, D., Javeri. J. (2018). Effect of process parameters in EDM of D2 steel and estimation of coefficient for predicting surface roughness. *Int. J. Mach. Mach. Mater*., vol. 20, 101–117, DOI: 10.1504/IJMMM.2018.090542

[21] Sonawane, S.A., Ronge, B.P., Pawar. P.M. (2019). Multi-characteristic optimization of WEDM for Ti-6Al-4V by applying grey relational investigation during profile machining. *J. Mech. Eng. Sci*., vol. 13, 6059–6087, DOI: 10.15282/jmes.13.4.2019.22.0478

[22] Doreswamy, D., Shreyas, D.S., Bhat. S.K. (2022). Optimization of Material Removal Rate, Surface Roughness and Kerf Width in Wire-ED Machining of Ti-6Al-4V Using RSM and Grey Relation. *Int J Eng, Trans B: Appl*., vol. 35, no. 11, 2247-2255, DOI: 10.5829/IJE.2022.35.11B.20

[23] Phate, M.R., Toney, S.B., Phate. V.R. (2021). Multi-parametric Optimization of WEDM Using Artificial Neural Network (ANN)-Based PCA for Al/SiCp MMC. *J. Inst. Eng. India Ser. C*., vol. 102, 169–181, DOI: 10.1007/s40032-020-00615-1

[24] Sharma, S.S., Kini, A., Shankar, G., Rakesh, T.C., Chaitanya, K., Shettar. M. (2018). Tensile fractography of artificially aged Al6061-B4C composites. *J Mech Eng Sci*., vol. 12, no. 3, 3866-3875, DOI: 10.15282/jmes.12.3.2018.8.0339

[25] Gruzleski, J.E., Closset. B.M. (1990). *The Treatment of Liquid Aluminum-Silicon Alloys*. American Foundrymen's Society, Incorporated, 172-175, Schaumburg.

[26] Perumal, A., Kailasanathan, C., Stalin, B., Kumar, S.S., Rajkumar, P.R., Gangadharan, T., Venkatesan, G., Nagaprasad, N., Dhinakaran, V., Krishnaraj, R. (2022). Multiresponse Optimization of Wire Electrical Discharge Machining Parameters for Ti-6Al-2Sn-4Zr-2Mo (α-β) Alloy Using Taguchi-Grey Relational Approach. *Advances in Materials Science and Engineering*, vol. 2022, 6905239, DOI: 10.1155/2022/6905239

[27] Raju, K., Balakrishnan, M., Priya, C.B., Sivachitra, M., Rao, D.N. (2022). Parametric Optimization of Wire Electrical Discharge Machining in AA7075 Metal Matrix Composite. *Advances in Materials Science and Engineering*, vol. 2022, 4438419, DOI: 10.1155/2022/4438419

[28] Deepak, D., Davim, J.P. (2019). Multi-Response Optimization of Process Parameters in AWJ Machining of Hybrid GFRP Composite by Grey Relational Method. *Procedia Manufacturing*, vol. 35, 1211-1221, DOI: 10.1016/j.promfg.2019.07.021

Paper submitted: 11.05.2023.

Paper accepted: 11.10.2023.